Characterization Tests of the Nb3Sn Cable-in-conduit Conductors for Se.C.R.E.T.S.

Pierluigi Bruzzone, Alexander Shikov, Alexandra Vorobieva, Victor Sytnikov, Arend Nijhuis, Werner Specking

***Abstract*—Two Nb_3Sn cable-in-conduit conductors have been procured for Se.C.R.E.T.S. (Segregated Copper Ratio Experiment on Transient Stability). The two conductors are identical in the fractional cross sections. The only difference is the location of the copper stabilizer, included either as segregated copper wires or as a copper shell in the superconducting strands. A number of characterization tests, on individual strands and cabled conductors, have been carried out to establish a solid data base for the assessment of the results in the main experiment.**

***Index terms*— Nb_3Sn cable-in-conduit, critical current, ac losses**

I. INTRODUCTION

The SeCRETS task is a crucial experiment on the role of the segregated copper in Nb_3Sn cable-in-conduit conductors [1]. A bifilar, single layer winding is inserted in the bore of the SULTAN test facility, at background field up to 11 *T*, operating current up to 12 *kA*, superimposed transverse pulse field to generate transient disturbances simulating the plasma disruption in a fusion magnet. The winding is made of two Nb_3Sn cable-in-conduit conductors, series connected, identical except the location of the copper stabilizer. The effectiveness of the segregated copper can be assessed comparing the stability performance of the two conductors. The use of segregated copper, and hence low copper fraction in the Nb_3Sn strands, allows substantial cost saving for large windings.

II. CONDUCTORS LAYOUT AND MANUFACTURE

The conductor A (without segregated copper) and B (with bundled copper wires), have been designed to have identical Cu and non-Cu cross sections, as well as identical size and void fraction. To simplify the procurement, the cable layout of conductor A is identical to the last-but-one cable stage of the high field ITER Model Coil conductor (CS1) [2], with all the stabilizing copper included in the superconducting strand cross section, Cu:non-Cu = 1.5. For conductor B, the Cu:non-Cu ratio in the superconducting strands is reduced to 1 and 16 copper cores are included in the cable, see Table 1.

The strands for both A and B are procured at VNIINM, Moscow, and are manufactured with the same method (bronze route). According to the strand supplier, the copper fraction can be easily adjusted over a broad range, starting from about 20%. The strands of both conductors, as well as the oxygen free copper cores in conductor B, are Cr plated at VNIIKP, Moscow. The thickness of the Cr layer is 2.5-2.8 μm.

The cabling and jacketing work is carried out at VNIIKP [3]. The 1st cable stage of conductor B has to be a 1+7 cable in order to obtain the same overall Cu and non-Cu cross section as in the 3x3 element of conductor A, with a similar strand diameter. The number of cable stages is three in B (four in A), see Fig.1. The last two cable stages and their pitches are identical in both conductors. A thin steel tape is wrapped on the final cable in opposite direction (left-hand) compared to the pitches of strand and cable (right hand). The production length of the cables is 58 *m* (A) and 69 *m* (B).

The jacket (identical for A and B) is assembled by TIG butt welding 6 *m* long units of seamless 316 L stainless steel pipes, 16 x 1 *mm*. The typical dimensional tolerance of the pipes is ± 0.1%. All the welds are leak tested. The cable is pulled through the welded, pre-assembled jacket with an insertion gap of 0.8 – 1.2 *mm*. Eventually, the conductor is compacted by a set of rollers to the final diameter of 14.54 ± 0.03 *mm*, providing a full engagement between cable and jacket. No thickening of the wall is observed during compaction. A number of straight sections are cut for ac losses and I_c tests. The remaining conductor lengths, ≈ 51 *m* for

TABLE 1. CONDUCTOR LAYOUT

	Conductor A	Conductor B
Cable configuration	3 x 3 x 4 x 4	(1+7) x 4 x 4
N of sc strands	144	112
N of Cu cores	0	16
Strand diameter	0.81 mm	0.82 mm
Cu:non-Cu in strand	1.5	1
Cu-core diameter	-	1.1 mm
non-Cu cross section	29.68 mm^2	29.57 mm^2
Cu cross section	44.52 mm^2	44.77 mm^2
Overall strand perimeter	0.366 m	0.343 m
SC strand perimeter	0.366 m	0.288 m
Twist pitches, mm	10, 48, 87, 120, 160	10, 61, 120,160
Nb_3Sn strand/m	0.66 kg/m	0.52 kg/m
Steel wrapping	25 x 0.065 mm, 14 mm pitch	
Jacket wall thickness	1. 01 ± 0.02mm	
Void fraction	≈ 37 %	
Conductor diameter	14.54 ± 0.03 mm	
Cable space diameter	12.54 ± 0.03 mm	

Manuscript received September 27, 1999
Pierluigi Bruzzone is with CRPP, CH 5232 Villigen-PSI, Switzerland (bruzzone@psi.ch), Alexander Shikov and Alexandra Vorobieva are with VNIINM, Moscow 123060, Russia, Victor Sytnikov is with VNIIKP, Moscow 111112, Russia, Arend Nijhuis is with University of Twente, 7500 AE Enschede, The Netherlands, Werner Specking is with FzK, 76021, Karlsruhe, Germany

1051-8223/00$10.00

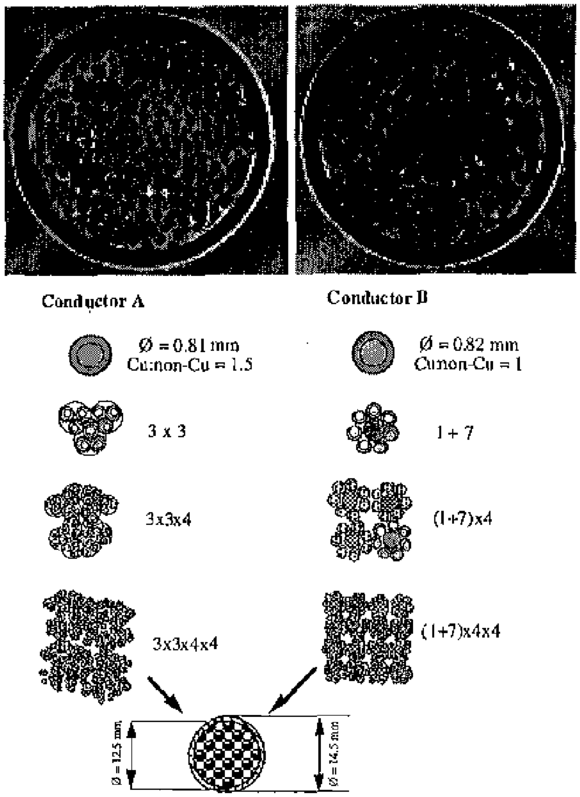

Fig. 1 Layout and cross section of the two cable-in-conduit conductors

both A and B, are wound on a drum, ø = 2 *m*, and leak tested.

III. Test Results

A. Strand Acceptance Tests

The strand for conductor B is obtained from four billet assemblies (no strand breakage). For conductor A, six billets have been used, with one strand breakage in three of them. The two-steps heat treatment on the acceptance specimens (one for each billet) is carried out in vacuum, 575 *C*/150 *hrs* and 600 *C*/ 200 *hrs*. The test results on $J_{cnon\text{-}Cu}$, hysteresis loss ± 3 *T* and RRR are summarized in Table 2. The tests are carried out at VNIINM, where the ITER strand bench mark test was also practiced in 1995 [4]. The RRR is defined for the overall strand, rather than for the Cu. The slightly lower values in strand B are due to the lower copper fraction [5].

TABLE 2. Summary Of Strand Tests Results

	Strand A	Strand B
Cu:non-Cu (range)	1.45 – 1.54	1.02
Average Cu:non-Cu in cable	1.50	1.02
$J_{c\,non\text{-}Cu}$ @ 12 T, 4.2 K, 0.1 μV/cm (range)	550 - 600	569 - 599
Average $J_{c\,non\text{-}Cu}$ in cable, A/mm^2	576	577
$J_{c\,non\text{-}Cu}$ from heat treatment witness specimen	520	501
Non-Cu hysteresis loss ± 3 T (range), mJ/cm^3	154 - 178	140 - 166
Average non-Cu hysteresis loss in cable	165	166
RRR in copper cores	-	> 100
RRR in strands (range)	101 – 116	88 – 105

Four I_c strand specimens have been attached to the SeCRETS winding as witness of the heat treatment in Ar gas. The critical current results (test at Univ. of Twente) are lower than measured at VNIINM, see Table 2. After checking the records of the heat treatment, the reason for this discrepancy (-7.4% for strand A and –11.9% for strand B) has not yet been clarified.

B. AC Losses In Cable-in-conduit Conductors

The ac losses were measured at Univ. of Twente on 480 *mm* long, straight sections of the cable-in-conduit conductors, heat treated together with the SeCRETS winding [1]. The test was carried out in the "virgin state", i.e. without any mechanical and electromagnetic load on the strand bundle. The applied sinus field had ± 0.4 *T* amplitude (no background field). The ac losses were measured by boil-off calorimetry. The results (loss curves) are gathered in Fig. 2 and Table 3.

The loss curves of conductor A and B, normalized to the superconducting strand volume (i.e. for the same non-Cu volume) converge to the same hysteresis loss, as expected from Table 2. The slope of B (circle) is smaller than A, suggesting smaller coupling currents loss. Normalizing the loss results to the overall cable volume (or to the cable length), the ac losses difference becomes almost a factor of two, mostly due to the effect of the segregated copper in conductor B. The lower loss in conductor B is likely due to smaller interfilament loss (due to the smaller copper fraction) and higher transverse resistance (see below).

The coupling loss in the SeCRETS conductor is smaller than expected in Nb_3Sn cable-in-conduit in "virgin state" [6]. A further loss decrease is expected in operation, due to the electromagnetic loads [7-8]: due to an increase of the interstrand resistance after loading, it is reasonable to expect that the coupling loss is eventually restricted to the interfilament loss. If the sc strands of A and B had the same $n\tau$, i.e. the same interfilament loss, the loss per conductor

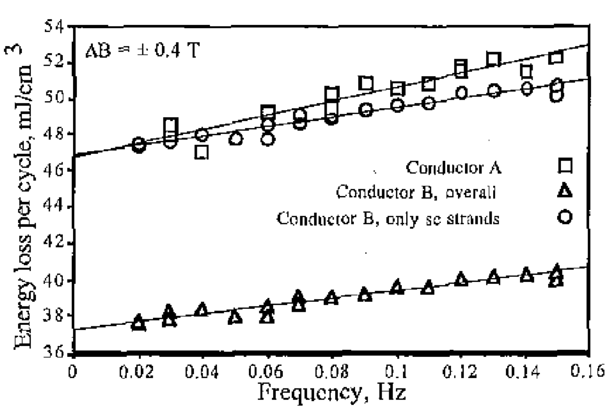

Fig. 2 AC losses of conductors A and B, normalized to the sc strand volume (square and circle) and to overall strand and Cu core (square and triangle)

TABLE 3. SUMMARY OF COUPLING LOSS RESULTS

	Conductor A	Conductor B
$n\tau$ (strand volume), ms	1.52	10.4
$n\tau$ (cable volume), ms	1.52	8.3
$n\tau \cdot A_{cable}$ (loss per unit length), ms·mm^2	0.205	0.112
Average R_c @ 0 T, nΩ·m	210	435
$n\tau \cdot R_c$, 10^{-9} s·Ω·m	3.6	3.2

unit length in A would be larger, compared to B, by a factor 1.27, which is the ratio of strand volume in A and B.

C. *Interstrand Resistance*

The interstrand contact resistance times length, R_c (Ω·m), is measured in 460 *mm* long, straight sections of conductor A and B at Univ. of Twente. At one end of the jacketed conductor, the cable bundle is opened and a number of strand pairs, see Fig. 3, is wired. The resistance is measured from the *V* vs. *I* curve at 0 and 1 *T* background field, with marginal increase at higher field. The resistance is constant over a broad range of dc current (up to 80 *A*).

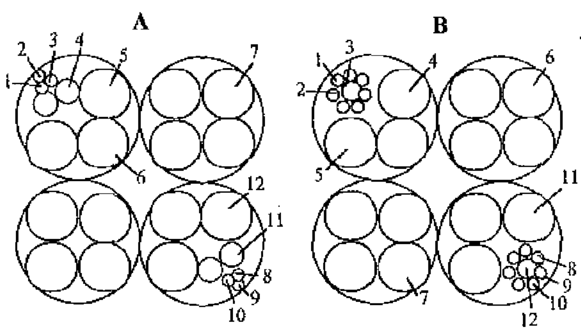

Fig. 3 Wiring schema for interstrand resistance specimens

The test results are gathered in Figs. 4 and 5. The resistance between adjacent strands in the first cable stage, as well as the average resistance in the bundle, is about a factor of two higher in conductor B. This may be explained considering that the interstrand resistance in a multistage cable is the results of the several zigzag paths of sc strands with different

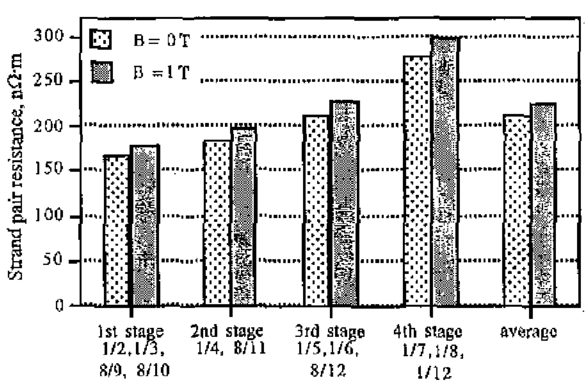

Fig. 4 Interstrand resistance in conductor A

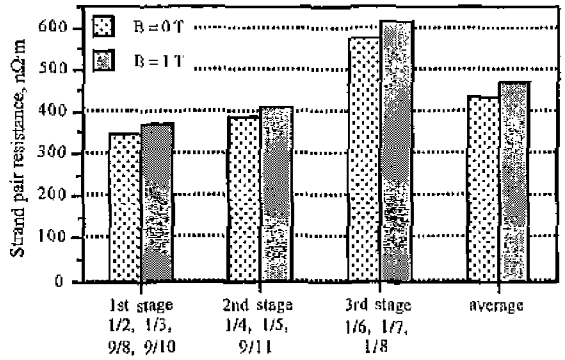

Fig. 5 Interstrand resistance in conductor B

angle in the bundle [9]: the larger number of sc strands and the larger average angle of strands in bundle in A (due to the larger number of cable stages) correlates with the lower transverse resistance in A. The Cr plated copper wires in conductor B do not contribute practically to the transverse conductance. The contact resistance of an individual strand crossover is assumed to be identical in A and B, due to the identical Cr plating.

The average interstrand resistance in the bundle correlates well with the coupling loss results. The product $n\tau \cdot R_c$ is identical, within the accuracy of the results (≈ 10%), for conductor A and B, see Table 3.

D. I_c *vs. Axial Strain On Cable-in-conduit Conductors*

Two straight cable-in-conduit conductor specimens, heat treated together with the SeCRETS winding, have been measured in the bath cooled split coils of the FBI facility at FzK, with field up to 14 *T*, current up to 10 *kA* and axial load up to 100 *kN* [10]. The critical current of the steel jacketed conductors was first measured vs. applied field at zero applied strain. Afterwards, at B = 14 *T*, I_c was measured as a function of the applied axial strain. The electrical field criterion for I_c is set at 1 *μV/cm*, with voltage taps spaced by 50 *mm*.

The $J_c(B)$ results for A and B conductors without applied

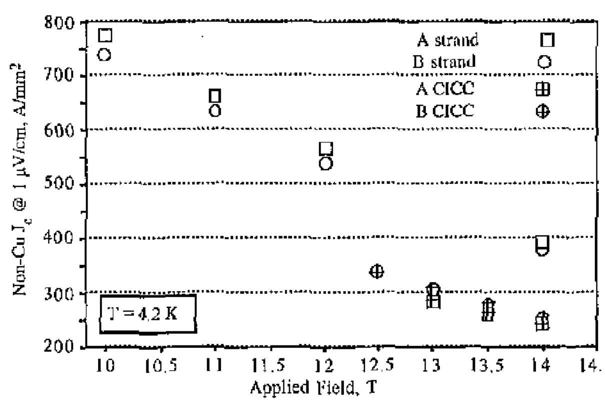

Fig. 6 Critical current density vs. field in CICCs and strands

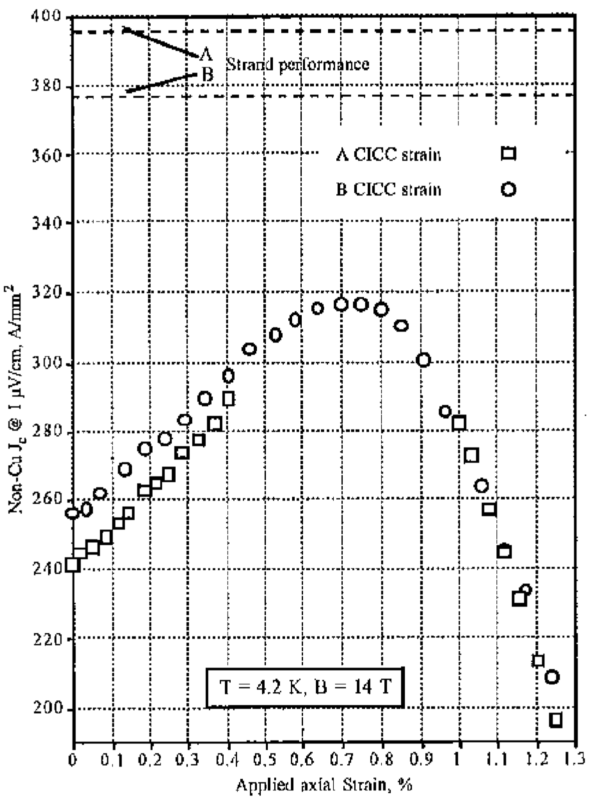

Fig. 7 Critical current vs. tensile strain at 14 T, for both A and B CICCs

strain are plotted in Fig. 6, together with the strand results at 1 $\mu V/cm$ (heat treatment witness specimens). The large difference between the results of strand and the steel jacketed conductors is due to the axial strain induced in the Nb_3Sn filaments by the steel shrinkage, in good agreement with [10].

The $J_c(\varepsilon)$ results are shown in Fig.7, were the full curve is measured only for the B conductor. The peak of J_c vs. ε occurs at $\varepsilon \approx 0.74\%$ applied strain, as it is expected in a steel jacketed conductor. However, the ratio of J_c without applied strain to the peak J_c is $J_{co}/J_{cm} = 0.81$, compared to 0.4-0.6 measured on similar cable-in-conduit conductors [10]. In other words, the peak current, J_{cm}, is smaller than expected and the whole data $J_c(\varepsilon)$ remain, at any strain, much smaller than the J_c measured on the strands.

The apparent contradiction of the scaling law may be explained with a bad cooling of the CICC specimens in the He bath. Initially, the cable void fraction is filled with liquid helium percolating through the tiny channels in the conductor section heavily compacted at the axial load grips. During the I_c test, the little power generated by the current transfer cannot be effectively removed by helium mass exchange due to the almost sealed conductor ends. Eventually, the cable space is cooled by conduction through the steel jacket and the operating temperature is substantially higher than the liquid Helium temperature.

The higher the current, the higher is the current sharing power and the operating temperature. This explains why the slope of I_c vs. ε in Fig. 7 is much smaller than predicted by the scaling law at constant temperature, although ε_{max} is in good agreement with the expected behavior. The crucial role of a good Helium mass exchange in the cable space has been verified on other CICC specimens in the FBI facility, where the I_c performance improved substantially after drilling large cooling holes in the jacket [11].

IV. Conclusion

Two cable-in-conduit conductors have been manufactured for the SeCRETS experiments to the same specifications, except the location of the copper stabilizer. The design requirements have been fulfilled. However, the strand specimens attached to the winding as heat treatment witness show a lower I_c performance compared to the acceptance test.

The coupling currents loss, measured on unloaded straight specimens (virgin state) is lower than expected for similar conductor layouts. The loss per length of the conductor with segregated copper wires is about half the one of the other conductor.

The interstrand resistance in the conductor with segregated copper, consistently with the coupling loss results, is about twice compared to the other conductor.

The critical currents of the two conductors are identical, at 0 applied load, within less than 5 %. However, the results of $I_c(\varepsilon)$ are affected by the non-isothermal test conditions.

References

[1] P. Bruzzone et al. *"SeCRETS, A stability experiment on the role of segregated copper in Nb₃Sn cable-in-conduit conductors"* Presented at MT-16 Conference

[2] P. Bruzzone et al. *"Conductor Fabrication for the ITER Model Coils"*, IEEE Mag 32, 2300 (1996)

[3] V. Sytnikov et al., *"Jacketing of 860 m ITER dummy CICC on Russian jacketing line"*, Proc. of MT 15, 1152, Beijing Oct. 1997, Science Press 1998

[4] P. Bruzzone et al. *"Bench mark testing of the Nb₃Sn strands for the ITER Model Coils"*, Adv. Cryog. Eng. (Mat) 42 B, 1351 (1996)

[5] A. Vorobieva et al., *"The study of Cu fraction influence on Nb₃Sn strand for ITER performance"* Presented at MT-16 Conference

[6] P. Bruzzone et al., *"Contact resistance and coupling loss in cable-in-conduit of Cr plated Nb₃Sn strands"*, Proc. of MT 15, 1295, Beijing Oct. 1997, Science Press 1998

[7] A Nijhuis et al., *"The influence of the Lorentz force on the ac loss in sub-size cable-in-conduit conductors for ITER"*, IEEE Appl Supercon 7, 262 (1997)

[8] P. Bruzzone et al. *"Test results for the high field conductor of the ITER central solenoid model coil"*, To be published in Adv. Cryog. Eng. 45

[9] K. Kwasnitza, P. Bruzzone, *"Large ac losses in superconducting Nb₃Sn cable due to low transverse resistance"* Proc. of ICEC 11, 515, Berlin 1986

[10] W. Specking, J-L. Duchateau, *"Improvement of I_c in Nb₃Sn conductors by reduction of axial pre-stress"*, IEEE Appl Supercon 5, 845 (1995)

[11] W. Specking, personal communication.